

# Multiphasic modelling of thrombus formation and growth based on the Theory of Porous Media

Ishan Gupta<sup>1,\*</sup> and Martin Schanz<sup>1,\*\*</sup>

<sup>1</sup> Institute of Applied Mechanics, Graz University of Technology, Technikerstraße 4, 8010 Graz, Austria

Aortic dissection (AD) has a high mortality rate. 40% of the people with Type B Aortic Dissection do not live for more than a month. The prognosis of Aortic Dissection is quite challenging leading to an interest in computational methods to help with the decision-making process for the treatment. The Theory of Porous Media (TPM) provides an excellent framework to describe the multiphasic structure of the thrombus. The whole aggregate is divided into solid, liquid and nutrient constituents. We assume the constituents to be materially incompressible, the whole aggregate to be fully saturated and under isothermal conditions. The balance equations of the constituents have coupling terms, also known as production terms, which take care of the interactions between the different phases. The volume fractions define the constituents. Therefore, the regions with thrombus are determined using the solid volume fraction. Darcy's law describes the flow of fluid in the porous media. We present the set of equations and a numerical example for thrombosis in Type B Aortic Dissection. We implement the equations in PANDAS, a finite element package designed to solve strongly coupled multiphase porous media problems.

© 2023 The Authors. *Proceedings in Applied Mathematics & Mechanics* published by Wiley-VCH GmbH.

## 1 Introduction

The aorta is one of the essential arteries in the body. The heart pumps the blood from the left ventricle into the aorta via the aortic valve, which opens and closes with each heartbeat to allow a one-way blood flow. Aortic dissection begins when the tear occurs in the inner layer (intima) of the aortic wall. This tear allows the blood to flow between the inner and middle layers causing them to separate (dissect). This second blood-filled channel is called the false lumen, where thrombosis occurs, see Figure 1. The tear can occur due to high blood pressure leading to increased stress on the aortic wall, weakening of the wall, pre-existing aneurysm or defects in the aortic valve. Approximately 75% of Type B Aortic Dissection (TBAD) patients have hypertension [1, 2].

Aortic dissection's short-term and long-term diagnosis remains unclear [3–6]. This led to an interest in computational methods to understand the formation and growth of thrombus. Blood clotting or coagulation is the process which prevents excessive bleeding by forming a spatial structure called a thrombus which consists of small blood cells (platelets) and fibrous protein (fibrin). The formation of a thrombus involves a complex sequence of biochemical reactions [7, 8]. Therefore, we use a macroscopic continuum-mechanical approach of the Theory of Porous Media (TPM) which provides an excellent framework to describe the complex microstructure of the multiphasic thrombus [9, 10]. The theory of mixtures was continuously improved and developed to the current understanding of the TPM by de Boer & Ehlers [11], and Ehlers [12, 13].

Chemical, mechanical, genetic, and metabolic factors drive the growth process of the thrombus. The model description is challenging due to the lack of detailed knowledge and parameters to quantify the influence of different factors. However, the effects of the blood velocity and the nutrients on the growth of thrombus are well-researched [14–16]. Therefore, we present a velocity and nutrient concentration-induced growth model based on the TPM. We treat the highly coupled set of differential equations within the framework of the standard Galerkin procedure and implement the weak forms in the nonlinear finite element solver PANDAS.

## 2 Theory of Porous Media

The Theory of Porous Media provides an excellent framework to macroscopically describe the complicated microstructure of the thrombus without knowing its detailed geometry. Therefore, a representative elementary volume (REV) is locally defined, where the individual constituents are considered to be in a state of ideal disarrangement. Using the real or virtual averaging processes over the REV, the micro-scale information of the overall aggregate and its constituents are homogenised to macro-scale quantities. For the investigated porous body, the immiscible parts lead to a triphasic aggregate  $\varphi$  consisting of solid  $\varphi^S$  (subendothelial collagen, activated platelets, fibrin, wall cells), which is saturated by fluid  $\varphi^F$ . The fluid itself consists of nutrients  $\varphi^N$  (deactivated platelets, clotting factors) and liquid  $\varphi^L$  (blood minus the nutrients and activated platelets), see Figure 2.

\* Corresponding author: e-mail ishan.gupta@tugraz.at

\*\* e-mail m.schanz@tugraz.at



This is an open access article under the terms of the Creative Commons Attribution-NonCommercial License, which permits use, distribution and reproduction in any medium, provided the original work is properly cited and is not used for commercial purposes.

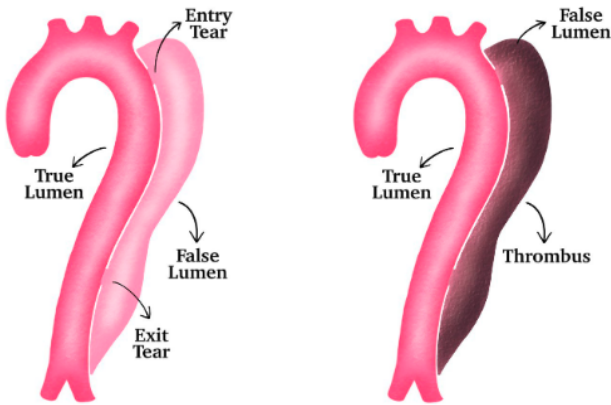


**Fig. 1:** Illustrations of the false lumen in TBAD (left) and formation of thrombus in false lumen (right) [17].

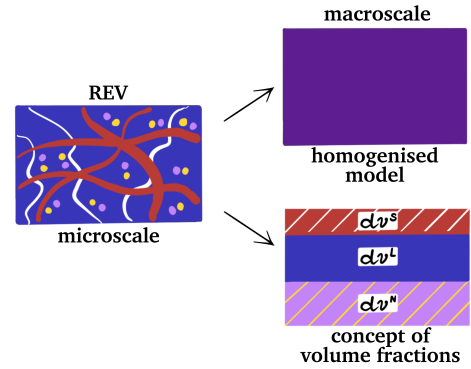


**Fig. 2:** REV of the microstructure of porous material (left), TPM macro-model obtained by volumetric homogenisation process (right) [10].

The volume fractions  $n^\alpha$  of the constituents  $\varphi^\alpha$ , where  $\alpha \in \{S, L, N\}$ , are defined as the local ratios of the respective partial volume elements  $dv^\alpha$  with respect to the bulk volume element  $dv$  of the overall aggregate  $\varphi$  as [10]

$$n^\alpha(\mathbf{x}, t) = \frac{dv^\alpha}{dv}, \quad \sum_{\alpha} n^\alpha(\mathbf{x}, t) = \sum_{\alpha} \frac{\rho^\alpha}{\rho^{\alpha R}} = 1, \quad (1)$$

where  $\mathbf{x}$  is the position vector in the current configuration at time  $t$ . The volume fractions  $n^\alpha$  need to fulfil the saturation constraint  $(1)_2$  permanently. Moreover, the partial density  $\rho^\alpha = dm^\alpha/dv$  of a constituent  $\varphi^\alpha$  can be related to its real density  $\rho^{\alpha R} = dm^\alpha/dv^\alpha$  via its volume fraction  $n^\alpha$   $(1)_2$ , where  $dm^\alpha$  is the constituent's mass element. Due to the volume fraction concept, all geometric and physical quantities, such as motion, deformation and stress, are defined in the total control space. Hence, they can be interpreted as the statistical average values of the real quantities.

### 3 Kinematics

The overall aggregate body  $B$  is defined as the connected manifold of material points  $P^\alpha$ . At any time  $t$ , material points  $P^\alpha$  of all the constituents  $\varphi^\alpha$  simultaneously occupy each spatial point  $\mathbf{x}$  of the current configuration. These particles proceed from different reference positions  $\mathbf{X}_\alpha$  at time  $t = t_o$ , which leads to individual motion, velocity  $\mathbf{x}'_\alpha$  and acceleration  $\mathbf{x}''_\alpha$  fields for each constituent

$$\mathbf{x} = \chi_\alpha(\mathbf{X}_\alpha, t), \quad \mathbf{x}'_\alpha = \frac{d\chi_\alpha(\mathbf{X}_\alpha, t)}{dt}, \quad \mathbf{x}''_\alpha = \frac{d^2\chi_\alpha(\mathbf{X}_\alpha, t)}{dt^2}. \quad (2)$$

Moreover, a unique inverse motion function  $\chi_\alpha^{-1}$  needs to exist for the motion function  $\chi_\alpha$  to be unique. The necessary and sufficient condition for this is the existence of non-singular jacobian  $J_\alpha$

$$\mathbf{X}_\alpha = \chi_\alpha^{-1}(\mathbf{x}, t), \quad \text{if} \quad J_\alpha := \det \frac{\partial \chi_\alpha}{\partial \mathbf{X}_\alpha} \neq 0, \quad (3)$$

where  $\det(\cdot)$  denotes the determinant operator. Moreover, the material deformation gradient  $\mathbf{F}_\alpha$  and its inverse  $\mathbf{F}_\alpha^{-1}$  are defined as  $\mathbf{F}_\alpha = \partial \chi_\alpha(\mathbf{X}_\alpha, t)/\partial \mathbf{X}_\alpha =: \text{Grad}_\alpha \mathbf{x}$  and  $\mathbf{F}_\alpha^{-1} = \partial \chi_\alpha^{-1}(\mathbf{x}, t)/\partial \mathbf{x} = \text{grad} \mathbf{X}_\alpha$  respectively. Here,  $\text{Grad}_\alpha(\cdot) = \partial(\cdot)/\partial \mathbf{X}_\alpha$  and  $\text{grad}(\cdot) = \partial(\cdot)/\partial \mathbf{x}$ . During deformation, the jacobian  $J_\alpha$  is restricted to  $J_\alpha = \det F_\alpha > 0$ . For scalar field functions  $\Psi$ , the material time derivative is defined as  $\Psi'_\alpha(\mathbf{x}, t) = \partial \Psi / \partial t + \text{grad} \Psi \cdot \mathbf{x}'_\alpha$ .

### 4 Balance equations

The balance equations for porous media are taken from the balance equations of the constituents  $\varphi^\alpha$  in mixture theory. The local equations of the balance of mass, the balance of momentum and the balance of moment of momentum for the constituents  $\varphi^\alpha$  read respectively as

$$(\rho^\alpha)'_\alpha + \rho^\alpha \text{div} \mathbf{x}'_\alpha = \hat{\rho}^\alpha, \quad \rho^\alpha \mathbf{x}''_\alpha = \text{div} \mathbf{T}^\alpha + \rho^\alpha \mathbf{b}^\alpha + (\hat{\mathbf{p}}^\alpha - \hat{\rho}^\alpha \mathbf{x}'_\alpha), \quad \mathbf{T}^\alpha = (\mathbf{T}^\alpha)^T. \quad (4)$$

In equations (4),  $\text{div}(\cdot)$  denotes the spatial divergence operator,  $\mathbf{T}^\alpha$  is the partial Cauchy stress tensor and  $\mathbf{b}$  is the external volume force per unit mass.  $\hat{\rho}^\alpha$  represents the total mass production accounting for mass exchange or phase transitions between the constituents  $\varphi^\alpha$ . The total momentum production  $\hat{\mathbf{p}}^\alpha = \hat{\mathbf{s}}^\alpha + \hat{\rho}^\alpha \mathbf{x}'_\alpha$  contains the direct momentum exchange  $\hat{\mathbf{s}}^\alpha$

resulting from the interaction force between the constituents  $\varphi^\alpha$  as well as indirect parts resulting from the mass exchange  $\hat{\rho}^\alpha$ . The total production terms are restricted by

$$\hat{\rho}^S + \hat{\rho}^L + \hat{\rho}^N = 0, \quad \hat{\mathbf{p}}^S + \hat{\mathbf{p}}^L + \hat{\mathbf{p}}^N = \mathbf{0}. \tag{5}$$

### 5 Assumptions

The system is investigated under the condition that all the constituents  $\varphi^\alpha$  are materially incompressible ( $\rho^{\alpha R} = \text{const.}$ ). This leads to the conclusion that volumetric deformations are only a result of a change in volume fractions  $n^\alpha$ . Moreover, the nutrient and the liquid phases are assumed to be in the fluid phase. Therefore, both phases are assigned the same velocity  $\mathbf{x}'_\alpha$  and pressure  $p^\alpha$

$$\mathbf{x}'_N = \mathbf{x}'_L = \mathbf{x}'_F, \quad p^N = p^L = p. \tag{6}$$

We assume that the liquid phase is not involved in the mass exchange. Using this assumption and equation (5)<sub>1</sub>

$$\hat{\rho}^L = 0 \quad \longrightarrow \quad \hat{\rho}^S = -\hat{\rho}^N. \tag{7}$$

Furthermore, only isothermal processes are considered, energy transfer due to chemical reactions is neglected, accelerations are excluded, and the internal structure of the thrombus is considered to be isotropic.

### 6 Constitutive modelling

The saturation condition (1)<sub>2</sub>, in addition, restricts the motion of incompressible constituents. Therefore, the set of unknown quantities should be extended by the Lagrange multiplier  $p$ , which is identified as a pore pressure. Considering saturation condition, the evaluation of entropy inequality in analogy to Coleman and Noll [18], and referring to de Boer [10] and Ricken [19], we get restrictions for the constitutive relations of  $\mathbf{T}^\alpha$ ,  $\hat{\mathbf{p}}^S$  and  $\hat{\rho}^S$ .

#### 6.1 Stress

The dependency of the Helmholtz free energy  $\psi^\alpha$  for the solid, liquid and nutrient phases is considered as

$$\psi^S = \psi^S\{n^S, \mathbf{C}_S\}, \quad \psi^L = \psi^L\{-\}, \quad \psi^N = \psi^N\{-\}, \quad \text{where } \mathbf{C}_S = \mathbf{F}_S^T \mathbf{F}_S. \tag{8}$$

We obtain the following constitutive relations for the stress with the above considerations, entropy inequality, equation (6), and equation (1)<sub>2</sub>.

$$\begin{aligned} \mathbf{T}^S &= -n^S p \mathbf{I} - (n^S)^2 \rho^{SR} \frac{\partial \psi^S}{\partial n^S} \mathbf{I} + \mathbf{T}_E^S, \quad \text{where } \mathbf{T}_E^S = 2\rho^S \mathbf{F}_S \frac{\partial \psi^S}{\partial \mathbf{C}_S} \mathbf{F}_S^T \\ \mathbf{T}^F &= \mathbf{T}^L + \mathbf{T}^N = -(n^L + n^N) p \mathbf{I} = -n^F p \mathbf{I}, \\ \mathbf{T} &= \mathbf{T}^S + \mathbf{T}^F = \mathbf{T}_E^S - (n^S)^2 \rho^{SR} \frac{\partial \psi^S}{\partial n^S} \mathbf{I} - p \mathbf{I}, \end{aligned} \tag{9}$$

where  $\mathbf{I}$  is the second-order identity tensor. The free energy function can be constructed in the following way

$$\psi^S = \left( \frac{n^S}{n_{OS}^S} \right)^n \frac{1}{\rho_{OS}^S} \left\{ \frac{\mu^S}{2} (I_1 - 3) - \mu^S \ln J_S + \lambda^S \frac{1}{2} (\ln J_S)^2 \right\}, \tag{10}$$

where  $\mu^S$  and  $\lambda^S$  are the macroscopic Lamé constants and  $(\cdot)_{OS}^{(\cdot)}$  represents the initial value of  $(\cdot)$  with respect to the solid reference configuration.  $I_1 := \text{tr } \mathbf{C}_S$  represents the first principal invariant of  $\mathbf{C}_S$ . From (9) and (10), the effective solid Cauchy stress can be obtained

$$\mathbf{T}_E^S = \left( \frac{n^S}{n_{OS}^S} \right)^{(n+1)} \left\{ \mu^S (\mathbf{B}_S - \mathbf{I}) + \lambda^S (\ln J_S) \mathbf{I} \right\}, \quad \text{where } \mathbf{B}_S = \mathbf{F}_S \mathbf{F}_S^T. \tag{11}$$

#### 6.2 Filter Velocity

The seepage velocity  $\mathbf{w}_{FS} = \mathbf{x}'_F - \mathbf{x}'_S$  determines the motion of the fluid in relation to the solid. The interaction forces,  $\hat{\mathbf{p}}^F = \hat{\mathbf{p}}^L + \hat{\mathbf{p}}^N = -\hat{\mathbf{p}}^S$ , connect the motions of both solid and fluid. From the evaluation of entropy inequality, we obtain the following relation

$$\hat{\mathbf{p}}^F = p \text{grad } n^F + \mathbf{S}_F \mathbf{w}_{FS}, \tag{12}$$

where  $\mathbf{S}_F$  is the permeability tensor between the solid and fluid. Using (12), (4)<sub>2</sub>,  $\mathbf{S}_F = \alpha_{FS} \mathbf{I}$  for isotropic material, and rearranging the equation, we get

$$n^F \mathbf{w}_{FS} = \frac{(n^F)^2}{\alpha_{FS}} \left( -\text{grad } p + \rho^{FR} \mathbf{b} - \frac{\hat{\rho}^F}{n^F} \mathbf{x}'_S \right), \quad \frac{(n^F)^2}{\alpha_{FS}} = \left( \frac{n^F}{n_{OS}^F} \right)^m \frac{k_{OS}^F}{\gamma^{FR}} = \left( \frac{n^F}{n_{OS}^F} \right)^m \frac{K_{OS}^S}{\mu^{FR}}. \quad (13)$$

The material parameter  $\alpha_{FS}$  can be described either by using initial Darcy's permeability of fluid  $k_{OS}^F$  [m/s] and effective fluid weight  $\gamma^{FR}$  [N/m<sup>3</sup>] or by using initial intrinsic permeability of solid  $K_{OS}^S$  [m<sup>2</sup>] and dynamic fluid viscosity  $\mu^{FR}$  [Ns/m<sup>2</sup>], see (13)<sub>2</sub>, where  $m$  is a dimensionless parameter which accounts for the change of permeability [10, 20]. From equations (7) and (13), we finally get the following relation for seepage velocity

$$n^F \mathbf{w}_{FS} = - \left( \frac{n^F}{n_{OS}^F} \right)^m \frac{K_{OS}^S}{\mu^{FR}} \left( \text{grad } p - \rho^{FR} \mathbf{b} - \frac{\hat{\rho}^S}{n^F} \mathbf{x}'_S \right). \quad (14)$$

### 6.3 Mass exchange

According to (7), the mass exchange occurs between the solid and nutrient phases  $\hat{\rho}^S = -\hat{\rho}^N$ . No expert knowledge is available for the formulation of free energy functions of liquid and nutrient phases. Therefore, following the evaluation of the entropy inequality and using the postulations proposed by Ricken [19, 20], the mass supply term of the solid phase is formulated.  $\hat{\rho}^S$  [kg/m<sup>3</sup> s] is postulated as a function of  $\mathbf{w}_{FS}$  and  $n^N$

$$\hat{\rho}^S(\mathbf{w}_{FS}, n^N) = \mathcal{C} \hat{\rho}_{\mathbf{w}_{FS}}^S \hat{\rho}_{n^N}^S, \quad \hat{\rho}_{\mathbf{w}_{FS}}^S(\mathbf{w}_{FS}) = \exp \left\{ -\frac{\|\mathbf{w}_{FS}\|^2}{\beta_1} \right\}, \quad \hat{\rho}_{n^N}^S(n^N) = -\exp \{ -(n^N)^2 \beta_2 \} + 1, \quad (15)$$

where  $\mathcal{C}$  represents the maximum mass exchange,  $\beta_1$  and  $\beta_2$  are the material parameters reflecting the dependence of mass exchange rate on the seepage velocity and nutrient volume fraction, see Figure 3.

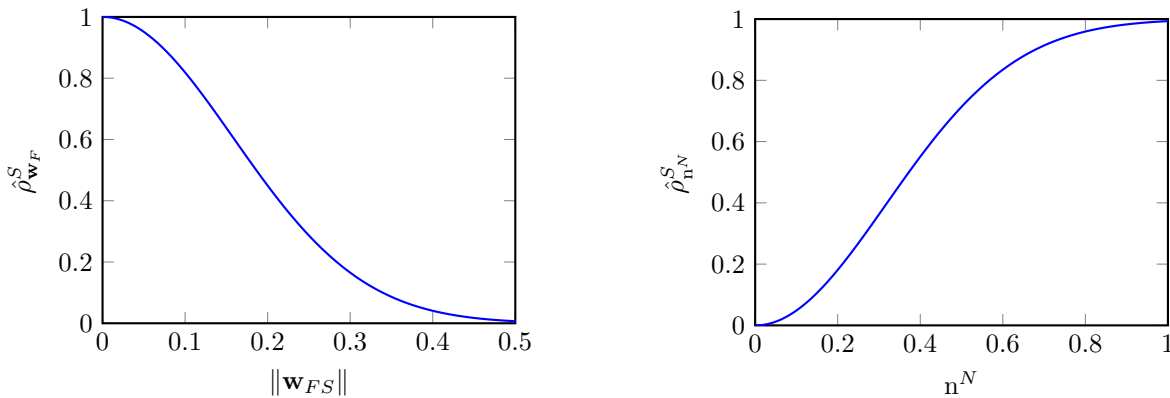


**Fig. 3:** Mass exchange rate dependence on the seepage velocity  $\mathbf{w}_{FS}$  and nutrient volume fraction  $n^N$ .

## 7 Numerical treatment and example

Considering the assumptions, balance equations, the saturation condition (1)<sub>2</sub> ( $n^L = 1 - n^S - n^N$ ), and constitutive relations from the preceding sections, we get a set of four unknown independent variables

$$\mathcal{U} = \mathcal{U}(\mathbf{x}, t) = \{ \mathbf{u}_S, n^S, n^N, p \}, \quad (16)$$

where  $\mathbf{u}_S$  is the displacement of the solid phase. Once this is concluded, the weak formulation for the governing equations is formulated in the framework of the standard Galerkin procedure (Bubnov-Galerkin). We multiply the momentum balance of the mixture, volume balance of the mixture, volume balance of the solid and volume balance of the nutrients with the test functions  $\delta \mathbf{u}_S, \delta p, \delta n^S$  and  $\delta n^N$ , respectively. As a result, the weak formulation of the triphasic model reads

- Momentum balance of mixture:

$$\mathcal{G}_{\mathbf{u}_S} = \int_{\Omega} (\mathbf{T}) : \text{grad } \delta \mathbf{u}_S \, dv - \int_{\Omega} (\rho^S + \rho^F) \mathbf{b} \cdot \delta \mathbf{u}_S \, dv - \int_{\Omega} \hat{\rho}^S \mathbf{w}_{FS} \cdot \delta \mathbf{u}_S \, dv - \int_{\Gamma_t} \bar{\mathbf{t}} \cdot \delta \mathbf{u}_S \, da = 0, \quad (17)$$

- Volume balance of mixture:

$$\mathcal{G}_p = \int_{\Omega} \operatorname{div} \mathbf{x}'_S \delta p \, dv - \int_{\Omega} n^F \mathbf{w}_{FS} \cdot \operatorname{grad} \delta p \, dv + \int_{\Omega} \hat{\rho}^S \left( \frac{1}{\rho^{NR}} - \frac{1}{\rho^{SR}} \right) \delta p \, dv + \underbrace{\int_{\Gamma_q} n^F \mathbf{w}_{FS} \cdot \mathbf{n} \delta p \, da}_{:=q} = 0, \quad (18)$$

- Volume balance of solid:

$$\mathcal{G}_{n^S} = \int_{\Omega} (n^S)'_S \delta n^S \, dv + \int_{\Omega} n^S \operatorname{div} \mathbf{x}'_S \delta n^S \, dv - \int_{\Omega} \frac{\hat{\rho}^S}{\rho^{SR}} \delta n^S \, dv = 0, \quad (19)$$

- Volume balance of nutrients:

$$\begin{aligned} \mathcal{G}_{n^N} = & \int_{\Omega} \left( (n^N)'_S + n^N \operatorname{div} \mathbf{x}'_S - \frac{\hat{\rho}^N}{\rho^{NR}} \right) \delta n^N \, dv + \underbrace{\int_{\Omega} \operatorname{grad} n^N \cdot \operatorname{grad} \delta n^N \, dv}_{:=r} \\ & - \int_{\Omega} n^N \mathbf{w}_{FS} \cdot \operatorname{grad} \delta n^N \, dv + \int_{\Gamma_v} n^N \mathbf{w}_{FS} \cdot \mathbf{n} \delta n^N \, da = 0. \end{aligned} \quad (20)$$

In the weak formulation, from (17) - (20),  $\bar{\mathbf{t}}$  is the external total stress vector acting on the Neumann boundary  $\Gamma_{\bar{\mathbf{t}}}$ ,  $n^F \mathbf{w}_{FS} \cdot \mathbf{n}$  is the fluid mass efflux on the Neumann boundary  $\Gamma_q$  and  $n^N \mathbf{w}_{FS} \cdot \mathbf{n}$  is the nutrient mass efflux on the Neumann boundary  $\Gamma_v$ , where  $\mathbf{n}$  is the outward-oriented unit surface normal. An artificial diffusion term ( $r$ ) is added to the volume balance of nutrients (20) to stabilise the transport equation [21].

The weak forms of balance equations are implemented in FE package PANDAS. We use the Taylor Hood elements for spatial discretisation, where we use the quadratic shape functions for  $\mathbf{u}_S$  and linear shape functions for  $p$ ,  $n^S$ , and  $n^N$ . Furthermore, the implicit Euler time-integration method is used. In this two-dimensional numerical example, we simulate the formation and growth of thrombus in TBAD. The geometry in the figure represents the false lumen where the mesh has 560 elements. It consists of a solid matrix filled with fluid. The fluid is allowed to leave at the exit tear. The rest of the boundaries are undrained surfaces. A boundary condition is applied for the fluid mass efflux  $q$  on the Neumann boundary  $\Gamma_q$  at the entry tear. Also, the volume fraction of the nutrients  $n^N$  is fixed at the entry tear. The bottom and the right edges are fixed in the  $y$  and  $x$  directions, respectively, see Figure 4. Moreover, the simulation is performed with a time step size of 10 seconds. The material parameters are given in Table 1 [19, 20, 22].

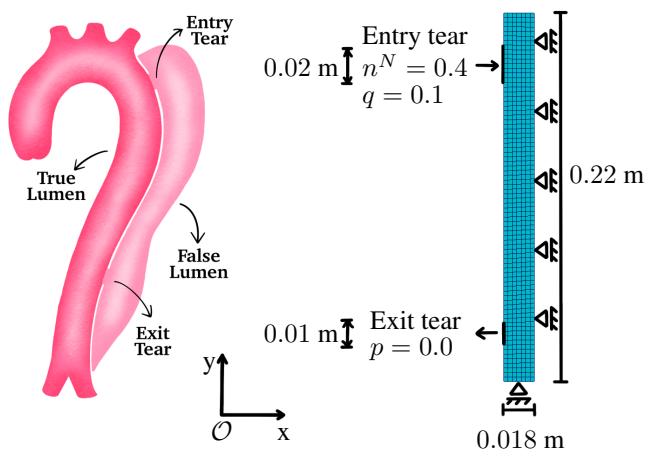
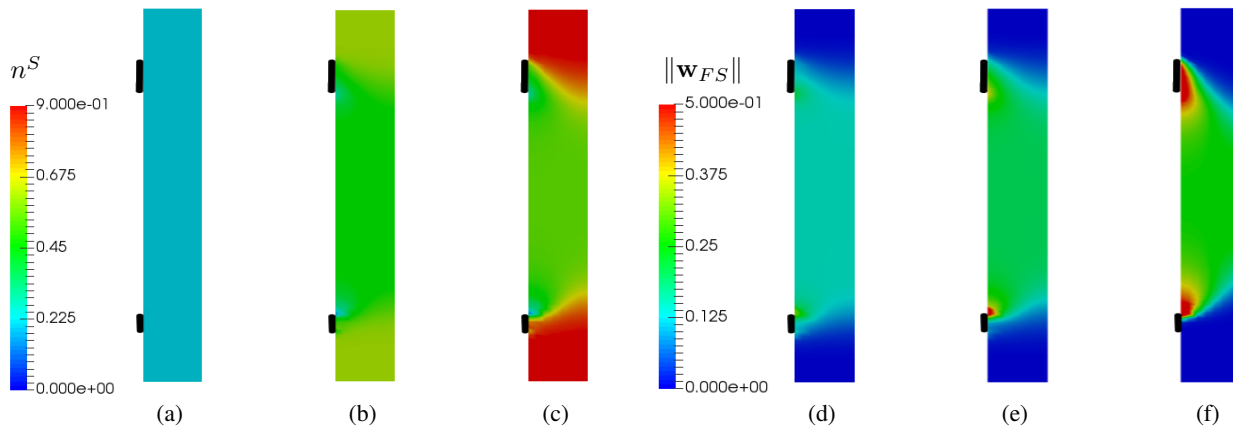


Fig. 4: Boundary conditions and discretization of false lumen.

Parameter	Value	Unit
$\lambda^S$	0.0	$N/m^2$
$\mu^S$	$1 \times 10^5$	$N/m^2$
$\mu^{FR}$	$1 \times 10^{-3}$	$Ns/m^2$
$k_{OS}^F$	$1 \times 10^{-6}$	$m/s$
$C$	$5 \times 10^{-2}$	$kg/sm^3$
$\rho^{SR}$	$2 \times 10^3$	$kg/m^3$
$\rho^{FR}$	$1 \times 10^3$	$kg/m^3$
$\rho^{NR}$	$2 \times 10^3$	$kg/m^3$
$n_{OS}^S$	0.2	-
$n_{OS}^N$	0.4	-
$\beta_1$	0.05	-
$\beta_2$	5.0	-

Table 1: Parameters for thrombus growth.

In the example of thrombosis over a period of a week, Figure 5, the growth of the thrombus can be seen at different stages in time. The entry and exit tears are marked in the figure. At time  $t = 0$ , the whole region has an initial solid volume fraction of 0.2 because of the presence of subendothelial collagen, wall cells and activated platelets on the formation of the false lumen. The fluid enters through the entry tear and leaves through the exit tear. As a result, the seepage velocity is high in the middle region and low in the false lumen's top and bottom regions. Also, it increases with time because of the less space available, see Figure 5 (right). Due to the presence of nutrients and following the mass exchange formulation (15), the process of thrombus formation begins, which can be compared to the formation of a platelet plug during primary haemostasis. Thereafter, secondary haemostasis begins, forming a mesh by fibrin and platelets and a stable clot, lasting for a long period. We have considered that at  $n^S = 0.8$ , the thrombus is stable enough, and it increases further to form a permanent and stable solid plug following secondary haemostasis. The reader is referred to Mohan [23] for a detailed explanation of thrombosis. However, there is a singularity at the exit tear due to the sharp edges in the idealised geometry, which is a numerical artefact. (cf. Figure 5).



**Fig. 5:** Change in solid volume fractions  $n^S$  at time (a)  $t = 0$  hours, (b)  $t = 84$  hours and (c)  $t = 168$  hours (left). Norm of the seepage velocity at time (d)  $t = 0$  hours, (e)  $t = 84$  hours and (f)  $t = 168$  hours (right).

## 8 Conclusions

A triphasic model has been developed for the growth of the thrombus. The Theory of Porous Media (TPM) is used to develop a thermodynamically consistent model using a smeared model of solid and nutrient-rich fluid phases. The constitutive relations are proposed based on the restrictions obtained by evaluating the entropy inequality. The mass exchange between the solid and nutrient phase is formulated, which depends on the nutrient concentration and the seepage velocity.

There is a lack of availability of enough medical data and realistic parameters. However, the model can describe the thrombus formation and growth process using the chosen parameters. The model can be expanded based on further findings and could then be adapted for patient-specific cases.

**Acknowledgements** We gratefully acknowledge Graz University of Technology for the financial support of the Lead-project: Mechanics, Modeling and Simulation of Aortic Dissection.

## References

- [1] K. J. Cherry and M. D. Dake, *Comprehensive Vascular and Endovascular Surgery*(1), 517–531 (2009).
- [2] F. Terzi, S. Gianstefani, and R. Fattori, *Journal of Cardiovascular Medicine* **19**, e50–e53 (2018).
- [3] R. Erbel, F. Alfonso, C. Boileau, O. Dirsch, B. Eber, A. Haverich, H. Rakowski, J. Struyven, K. Radegran, U. Sechtem, J. Taylor, C. Zollkofer, W. W. Klein, B. Mulder, and L. A. Providencia, *European Heart Journal* **22**, 1642–1681 (2001).
- [4] A. Kumar and R. M. Allain, *Critical Care Secrets: Fifth Edition* pp. 204–211 (2012).
- [5] T. Luebke and J. Brunkwall, *AORTA Journal* **2**, 265 (2014).
- [6] T. T. Tsai, S. Trimarchi, and C. A. Nienaber, *European Journal of Vascular and Endovascular Surgery* **37**, 149–159 (2009).
- [7] A. Undas and R. A. Ariens, *Arteriosclerosis, thrombosis, and vascular biology* **31**(12) (2011).
- [8] A. S. Wolberg and R. A. Campbell, *Transfusion and apheresis science : official journal of the World Apheresis Association : official journal of the European Society for Haemapheresis* **38**(2), 15 (2008).
- [9] W. Ehlers, *Porous Media: Theory, Experiments and Numerical Applications* pp. 3–86 (2002).
- [10] R. de Boer, *Theory of Porous Media* (2000).
- [11] R. de Boer and W. Ehlers, *Theory of multicomponent continua and its application to problems of soil mechanics. pt. 1. theorie der mehrkomponentenkontinua mit anwendung auf bodenmechanische probleme. t. 1*, 1986.
- [12] W. Ehlers, *Continuum Mechanics in Environmental Sciences and Geophysics* pp. 313–402 (1993).
- [13] W. Ehlers, *Porous Media* pp. 3–86 (2002).
- [14] M. B. Zucker, *Methods in Enzymology* **169**(1), 117–133 (1989).
- [15] N. Begent and G. V. Born, *Nature* 1970 227:5261 **227**, 926–930 (1970).
- [16] I. V. Pivkin, P. D. Richardson, and G. Karniadakis, *Proceedings of the National Academy of Sciences of the United States of America* **103**(11), 17164 (2006).
- [17] C. A. Nienaber, S. Kische, H. Rousseau, H. Eggebrecht, T. C. Rehders, G. Kundt, A. Glass, D. Scheinert, M. Czerny, T. Kleinfeldt, B. Zipfel, L. Labrousse, R. Fattori, and H. Ince, *Circulation: Cardiovascular Interventions* **6**(8), 407–416 (2013).
- [18] B. D. Coleman and W. Noll, *The Foundations of Mechanics and Thermodynamics* pp. 145–156 (1974).
- [19] T. Ricken, A. Schwarz, and J. Bluhm, *Computational Materials Science* **39**(3), 124–136 (2007).
- [20] T. Ricken and J. Bluhm, *Arch Appl Mech* **80**, 453–465 (2010).
- [21] T. D. Santos, M. Morlighem, and H. Seroussi, *Geoscientific Model Development* **14**(5), 2545–2573 (2021).
- [22] X. Zheng, A. Yazdani, H. Li, J. D. Humphrey, and G. E. Karniadakis, *PLOS Computational Biology* **16**(4), e1007709 (2020).
- [23] H. Mohan, *Textbook of pathology* (Jaypee Brothers Medical Publishers, 2018).